

Towards Optimal Design of Time and Color Multiplexing Codes

Tsung-Han Chan^{1,2}, Kui Jia¹, Eliot Wycoff¹, Chong-Yung Chi², and Yi Ma^{3,4}

¹ Advanced Digital Sciences Center, Singapore

² Inst. Communications Eng., National Tsing Hua University, Taiwan

³ Microsoft Research Asia, Beijing, China

⁴ Dept. Elect. and Computer Eng., University of Illinois at Urbana-Champaign
{Th.chan,Chris.jia,Eliot.wycoff}@adsc.com.sg, mayi@microsoft.com

Abstract. Multiplexed illumination has been proved to be valuable and beneficial, in terms of noise reduction, in wide applications of computer vision and graphics, provided that the limitations of photon noise and saturation are properly tackled. Existing optimal multiplexing codes, in the sense of maximum signal-to-noise ratio (SNR), are primarily designed for time multiplexing, but they only apply to a multiplexing system requiring the number of measurements (M) equal to the number of illumination sources (N). In this paper, we formulate a general code design problem, where $M \geq N$, for time and color multiplexing, and develop a sequential semi-definite programming to deal with the formulated optimization problem. The proposed formulation and method can be readily specialized to time multiplexing, thereby making such optimized codes have a much broader application. Computer simulations will discover the main merit of the method— a significant boost of SNR as M increases. Experiments will also be presented to demonstrate the effectiveness and superiority of the method in object illumination.

Keywords: Multiplexing codes, maximum SNR, convex optimization.

1 Introduction

Optical multiplexing can be tracked back to the late 70s in the field of spectrometry [1], where a single detector simultaneously receives signals from different spectral bands which are specifically encoded. The goal of multiplexing is to improve signal-to-noise ratio (SNR) of the demultiplexed, single spectral band signals. An analogous multiplexing concept has been brought into the domain of computer vision and graphics by Schechner et al. in 2003 [2], where they illuminated objects by multiple sources from different directions and computationally demultiplexed the received images, attempting to acquire high-SNR, single-light source images. Such a multiplexing scheme was afterwards employed in applications, such as scene recovery [3], object relighting [4], fluorescence unmixing [5] and photometric stereo [6–8], and has been proved to improve SNR.

The SNR boost of single-light source images is anticipated to have a profound and immediate impact on the successes in computer vision applications.

For instance, in face recognition system [9], gathering face training images under arbitrary illuminations via multiplexing scheme would result in noise reduction and subsequently improve the recognition rate. In photometric stereo [6–8], estimating the surface normals of objects from the multiplexing-applied, single-light source images can substantially aid in object recognition and 3-D modeling. The above advantages are expected when there is only sensor noise involved. When the photon noise comes into play, multiplexing multiple light sources may become counterproductive [10]. Present efforts for designing multiplexing codes in the presence of both sensor noise and photon noise include the works in [10–12], but they are limited to time multiplexing system where the number of measurements (M) equals the number of illumination sources (N). Some questions may arise: How to design the multiplexing codes for the system not only applying time multiplexing but also color multiplexing? What we can gain from the multiplexing if the number of measurements M is more than the number of illumination sources N ?

Indeed, some existing works have utilized time and color multiplexing for various purposes [4, 7, 13, 14], but there is not much information on how the time and color multiplexing codes were designed. In this paper, we investigate the possibility of designing optimal time and color multiplexing codes, with $M \geq N$, for achieving maximum SNR in the demultiplexed images. We first formulate the code design problem as a constrained optimization problem, and it takes into account the presence of sensor noise and photon noise, as well as the saturation issue [11]. Since the formulated problem is non-convex, we propose to use a sequential convex programming to approximate the problem, where each subproblem is formulated as a semi-definite program and thus can be solved by any convex optimization solver. The proposed formulation and algorithm can be readily specialized to time multiplexing, thereby making such optimized codes have a much broader application. Simulations will discover the merits of our approach—a significant SNR boost when M increases, and requirement of $1/K$ measurements in time and color multiplexing for achieving equal performance when using time multiplexing, where K denotes the number of color channels; e.g., $K = 3$ for RGB color camera. Experiments are presented to demonstrate the effectiveness and superiority of the proposed approach in object illumination.

2 Background of Time Multiplexing

We briefly review the background of time multiplexing and some related works in this section. To start with, let us consider a scenario that a static object with Lambertian surfaces is illuminated by multiple, say N , diverse single light sources using time-multiplexed scheme, and each light source has its own direction from which the light source illuminates a surface patch of the object. Assuming there are N distinct multiplexed illuminations in total, the captured intensity value at pixel n can be represented by a linear superposition model:

$$\mathbf{x}[n] = \mathbf{A}\mathbf{s}[n] + \mathbf{v}[n], \quad n = 1, \dots, L, \quad (1)$$

where $\mathbf{x}[n] \in \mathbb{R}^N$ is a vector containing the captured light intensity for N different multiplexed illuminations at pixel n , $\mathbf{A} \in \mathbb{R}^{N \times N}$ is a time multiplexing matrix, $\mathbf{s}[n] = [s_1[n], \dots, s_N[n]]^T$ denotes a vector comprising intensities of the reflected light at the n th pixel, under different N single lighting conditions, $\mathbf{v}[n] \in \mathbb{R}^N$ is the measurement noise, and L is the total number of image pixels. The 1-dimensional pixel index n results from a vector transformation of 2-dimensional image coordinate.

Time multiplexing in (1) uses non-switching strategy, where the elements of the matrix \mathbf{A} are from 0 to 1, not restricted to 0 or 1; i.e., $\mathbf{0} \preceq \text{vec}(\mathbf{A}) \preceq \mathbf{1}_{NN}$, where \preceq denotes componentwise inequality for vectors or linear matrix inequality for matrices, $\text{vec}(\cdot)$ denotes vectorization operator, $\mathbf{1}_N$ is N -dimensional all-one vector, and $\mathbf{0}$ is all-zero vector of proper dimension. The extreme values 0 and 1 stand for the corresponding light source being completely turned off and turned on, respectively. The values of $\{\mathbf{s}[n]\}_{n=1}^L$ depend on object and light source relative position, orientation and visibility. In addition, the noise $\mathbf{v}[n]$ is assumed to be independent and identically distributed (i.i.d.), zero mean, with covariance matrix satisfying the affine noise model [4, 15]:

$$\Sigma_P = (\sigma^2 + P\rho^2)\mathbf{I}_N, \quad (2)$$

where σ^2 denotes the variance of the signal-independent sensor noise, ρ^2 denotes the variance of signal-dependent photon noise, \mathbf{I}_N is $N \times N$ identity matrix, and P is total energy of the activated light sources at each measurement. The value of P has a direct connection to the time multiplexing matrix \mathbf{A} , indicating the multiplexing power used in each measurement is equal to P ; i.e., $\mathbf{A}\mathbf{1}_N = P\mathbf{1}_N$.

A solution to recover the pixel values under various single-light source illuminations $\mathbf{s}[n]$, $n = 1, \dots, L$ is to multiply \mathbf{A}^{-1} to the multiplexed images $\mathbf{x}[n]$, $n = 1, \dots, L$:

$$\widehat{\mathbf{s}}[n] = \mathbf{A}^{-1}\mathbf{x}[n] = \mathbf{s}[n] + \mathbf{A}^{-1}\mathbf{v}[n], \quad n = 1, \dots, L. \quad (3)$$

From (3), it is obvious that the single-light source illumination $\mathbf{s}[n]$ can be estimated subject to some noise contamination $\mathbf{A}^{-1}\mathbf{v}[n]$. A question arises: Could someone make use of \mathbf{A} so as to demultiplex high quality $\widehat{\mathbf{s}}[n]$, or to minimize the effect of noise $\mathbf{A}^{-1}\mathbf{v}[n]$ in $\widehat{\mathbf{s}}[n]$. This is exactly the primary goal of the multiplexing, which attempts to devise the time multiplexing matrix \mathbf{A} such that the estimated single-light source illumination $\widehat{\mathbf{s}}[n]$ has maximum signal-to-noise ratio (SNR) [11], or equivalently,

$$\begin{aligned} \{\mathbf{A}^*, P^*\} &= \arg \min_{\mathbf{A} \in \mathbb{R}^{N \times N}, P \in \mathbb{R}} \text{Tr}((\mathbf{A}^T \Sigma_P^{-1} \mathbf{A})^{-1}) \\ \text{s.t.} \quad &\mathbf{0} \preceq \text{vec}(\mathbf{A}) \preceq \mathbf{1}_{NN}, \mathbf{A}\mathbf{1}_N = P\mathbf{1}_N, \end{aligned} \quad (4)$$

where $\text{Tr}(\cdot)$ is the trace operator. As compared to the scenario of single-source acquisition; i.e., $\mathbf{A} = \mathbf{I}_N$, the SNR gain of time multiplexing can be easily computed as

$$G_t = \sqrt{\frac{\text{Tr}(\Sigma_1)}{\text{Tr}((\mathbf{A}^*)^T \Sigma_{P^*}^{-1} \mathbf{A}^*)^{-1}}}, \quad (5)$$

where Σ_1 is given by (2) with setting $P = 1$. The SNR gain G_t can also be called as time multiplexing gain.

2.1 Related Works

In the following, we categorize previously related works based on conditions under which the methods for handling problem (4) were developed.

Absence of Photon Noise: Optical multiplexing technique was first investigated in the field of spectrometry [1]. The optimal multiplexing codes for problem (4) has been shown to be S-matrix [1, 2, 4] when the photon noise is absent; i.e., $\rho^2 = 0$. The S-matrix can be readily constructed based on Hadamard codes of length $N+1$ for some N such that $(N+1)/4$ is an integer. Hadamard multiplexing is switch multiplexed method, which completely turns on $P^* = (N+1)/2$ light sources at each measurement. Using Hadamard multiplexing, the time multiplexing gain is $G_t = (N+1)/(2\sqrt{N})$ [1]. Clearly, the more the number of illumination sources N , the more image quality we can gain using multiplexing.

Presence of Photon Noise: When photon noise comes into play, Hadamard multiplexing is not optimal anymore [6]. Mutting [10] looked into the effect of photon noise to Hadamard multiplexing, and derived new multiplexing codes, based on two-level autocorrelation sequences. These multiplexing codes have shown their advantages when there are photon noise, but they are only available for a very limit set of N and for limit range of noise variances $\{\sigma^2, \rho^2\}$. Thus, Ratner et al. [11] constructed new time multiplexing codes for any N and noise variances $\{\sigma^2, \rho^2\}$. They dealt with problem (4) for a given P using the projected gradient method, which may easily get stuck in the local optima during the solution search. Hence, they also devise a higher level optimization procedure for the method to escape from local optima [11]. After collecting all the optimal objective values of problem (4) for all the P 's, the optimal P^* was then selected as the one with minimum objective value.

Saturation: Another issue encountered in illumination multiplexing is saturation, and it may occur when the object is illuminated by numerous light sources. When the captured image intensity is saturated, meaning that the linear superposition model (1) is violated, one should either reduce the exposure time or decrease the total energy P for each measurement. [2, 4] has proved that the latter is better than the former. Thus, to counter saturation issue, Ratner et al. have added a constraint:

$$P \leq P_{\text{sat}}, \quad (6)$$

where P_{sat} is the threshold beyond which the captured image gets saturated.

Despite the success of the above methods, the present time multiplexing codes are limited to time multiplexing and the determined, multiplexing system (or $\mathbf{A} \in \mathbb{R}^{N \times N}$ is square). Some interesting questions may arise: Can the code design problem for time multiplexing be extended to that for time and color multiplexing? What if the multiplexing system can allow to capture more number of measurements? In the next section, we will formulate a maximum-SNR code

design problem for time and color multiplexing, where the multiplexing matrix is not limited to be square. Some advantages of employing, over-determined, time and color multiplexing system will be discovered and discussed therein.

3 Time and Color Multiplexing

Time and color multiplexing has been utilized for relighting [4], multi-spectral imaging [13], and capturing varying illumination conditions [7, 14], but none of them specifically elaborate how to optimally devise the codes for time and color multiplexing. In this section, we introduce the model of time and color multiplexing, and present how the codes for time and color multiplexing can be designed in a near-optimal way. As reported in [14], the captured time-multiplexing images of a static Lambertian object at RGB channels should fulfill the following linear superposition model:

$$\mathbf{x}_c[n] = \alpha_c[n]\mathbf{A}_c\mathbf{s}[n] + \mathbf{v}_c[n], \quad n = 1, \dots, L, \quad c \in \{r, g, b\} \quad (7)$$

where $\mathbf{x}_r[n], \mathbf{x}_g[n], \mathbf{x}_b[n] \in \mathbb{R}^M$ denote M -time multiplexed image intensity at pixel n , recorded via red, green, and blue channels, respectively, $\alpha_r[n], \alpha_g[n], \alpha_b[n] \in \mathbb{R}$ represent the illumination-independent, normalized RGB intensities of the material at image pixel n , satisfying $\alpha_r[n] + \alpha_g[n] + \alpha_b[n] = 1$, $n = 1, \dots, L$, $\mathbf{A}_r, \mathbf{A}_g, \mathbf{A}_b \in \mathbb{R}^{M \times N}$ are the time-multiplexing matrices for red, green, and blue channels, respectively, $\mathbf{s}[n] \in \mathbb{R}^N$ corresponds to various single-light source illuminations at pixel n , and $\mathbf{v}_r[n], \mathbf{v}_g[n], \mathbf{v}_b[n] \in \mathbb{R}^M$ denote the i.i.d. noise measured in RGB channels, respectively. The noise covariance matrices for RGB channels are usually diverse, depending on specification of the color camera used; i.e., $\Sigma_P^c = (\sigma_c^2 + P\rho_c^2)\mathbf{I}_M$, $c \in \{r, g, b\}$. Here, the number of time multiplexing M can be different from the number of illumination sources N . Also, the material colors and the noise covariance matrices can be practically acquired in camera calibration phase, and they are assumed to be known herein. The details of how to estimate those parameters can be referred to Section 5.1.

We first reformulate the model (7). Moving the effects of material colors $\alpha_r[n], \alpha_g[n], \alpha_b[n]$, $n = 1, \dots, L$ into noise, and staking RGB counterparts as a column vector, we obtain

$$\mathbf{y}[n] \triangleq \begin{bmatrix} \mathbf{x}_r[n]/\alpha_r[n] \\ \mathbf{x}_g[n]/\alpha_g[n] \\ \mathbf{x}_b[n]/\alpha_b[n] \end{bmatrix} = \begin{bmatrix} \mathbf{A}_r \\ \mathbf{A}_g \\ \mathbf{A}_b \end{bmatrix} \mathbf{s}[n] + \begin{bmatrix} \mathbf{v}_r[n]/\alpha_r[n] \\ \mathbf{v}_g[n]/\alpha_g[n] \\ \mathbf{v}_b[n]/\alpha_b[n] \end{bmatrix} \in \mathbb{R}^{3M} \quad (8)$$

$$= \mathbf{F}\mathbf{s}[n] + \mathbf{w}[n], \quad n = 1, \dots, L, \quad (9)$$

where $\mathbf{F} = [\mathbf{A}_r^T, \mathbf{A}_g^T, \mathbf{A}_b^T]^T \in \mathbb{R}^{3M \times N}$ is the time and color multiplexing matrix, and $\mathbf{w}[n] = [\mathbf{v}[n]_r^T/\alpha_r[n], \mathbf{v}[n]_g^T/\alpha_g[n], \mathbf{v}[n]_b^T/\alpha_b[n]]^T \in \mathbb{R}^{3M}$ is the noise having block diagonal covariance matrix

$$\mathbf{\Lambda}_P = \text{Bdiag} \left(\sum_{n=1}^L \frac{\Sigma_P^r}{\alpha_r^2[n]L}, \sum_{n=1}^L \frac{\Sigma_P^g}{\alpha_g^2[n]L}, \sum_{n=1}^L \frac{\Sigma_P^b}{\alpha_b^2[n]L} \right) \in \mathbb{R}^{3M \times 3M}, \quad (10)$$

thanks to i.i.d. property of the noise. Here, $\text{Bdiag}(\mathbf{C}_1, \dots, \mathbf{C}_N)$ denotes a block diagonal matrix with the diagonal blocks equal to $\mathbf{C}_1, \dots, \mathbf{C}_N$. The structure in (10) is for ease of presentation, and any correlation across RGB channels caused by Bayer filter and color interpolation will not change the optimization procedure (to be presented in Section 3.1) and the optimality of the yielded solution.

Assuming that $3M \geq N$, the unique recovery of single-source illumination $\mathbf{s}[n]$ from $\mathbf{y}[n]$ can be written as

$$\hat{\mathbf{s}}[n] = \mathbf{G}^T \mathbf{y}[n] = \mathbf{s}[n] + \mathbf{G}^T \mathbf{w}[n], \quad n = 1, \dots, L, \quad (11)$$

where $\mathbf{G} \in \mathbb{R}^{3M \times N}$ is a demultiplexing matrix such that $\mathbf{G}^T \mathbf{F} = \mathbf{I}_N$. Unlike the case of $3M = N$, where \mathbf{G} can be trivially determined as \mathbf{F}^{-1} , we herein consider \mathbf{G} is unknown and to be designed. Hence, the time and color multiplexing is to jointly devise \mathbf{F} and \mathbf{G} such that the SNR of $\hat{\mathbf{s}}[n]$ is maximum, which turns out to be equivalent to minimizing the noise power subject to all the constraints considered in (4):

$$\begin{aligned} \min_{\mathbf{F}, \mathbf{G} \in \mathbb{R}^{3M \times N}, P \in \mathbb{R}} \quad & \text{Tr}(\mathbf{G}^T \mathbf{\Lambda}_P \mathbf{G}) \\ \text{s.t.} \quad & \mathbf{G}^T \mathbf{F} = \mathbf{I}_N, \quad \mathbf{0} \preceq \text{vec}(\mathbf{F}) \preceq \mathbf{1}_{3MN}, \quad \mathbf{F} \mathbf{1}_N = P \mathbf{1}_{3M}. \end{aligned} \quad (12)$$

By the Lagrangian multiplier method [16], we can obtain the a closed-form solution \mathbf{G} for the above problem, in terms of \mathbf{F} and P , as follows:

$$\mathbf{G}^* = \mathbf{\Lambda}_P^{-1} \mathbf{F} (\mathbf{F}^T \mathbf{\Lambda}_P^{-1} \mathbf{F})^{-1}. \quad (13)$$

The details of how we derive (13) can be found in the Supplementary Material (SM)¹. Substituting (13) into (12) yields

$$\begin{aligned} \{\mathbf{F}^*, P^*\} = \arg \min_{\mathbf{F} \in \mathbb{R}^{3M \times N}, P \in \mathbb{R}} \quad & \text{Tr}((\mathbf{F}^T \mathbf{\Lambda}_P^{-1} \mathbf{F})^{-1}) \\ \text{s.t.} \quad & \mathbf{0} \preceq \text{vec}(\mathbf{F}) \preceq \mathbf{1}_{3MN}, \quad \mathbf{F} \mathbf{1}_N = P \mathbf{1}_{3M}. \end{aligned} \quad (14)$$

In comparison to straightforward time and color multiplexing; i.e., $3M = N$ and $\mathbf{F} = \mathbf{I}_N$, the gain of optimal time and color multiplexing can be defined as

$$G_{\text{tc}} = \sqrt{\frac{\text{Tr}(\mathbf{\Lambda}_1)}{\text{Tr}((\mathbf{F}^*)^T \mathbf{\Lambda}_P^{-1} \mathbf{F}^*)^{-1}}}, \quad (15)$$

where $\mathbf{\Lambda}_1$ is the noise covariance given by (10) with $P = 1$.

The objective function of problem (14) is highly non-convex. Directly handling this problem with any non-linear programming method could suffer from risk of local optimality. Though one may use Ratner's method [11,12] to tackle problem (14), it is limited to the case of square multiplexing matrix $3M = N$ and $\mathbf{\Lambda}_P = \beta \mathbf{I}_{3M}$ for any $\beta > 0$. In what follows, we propose to handle problem (14) of any $3M \geq N$ and $\mathbf{\Lambda}_P$ by sequential convex programming (SCP), where each subproblem involved in SCP is in form of semi-definite programming (SDP) and hence can be readily solved by convex optimization solvers [17].

¹ The SM can be downloaded at

<http://web.adsc.com.sg/perception/publications.html>.

3.1 Design of Time and Color Multiplexing Codes

To alleviate difficulties in solving problem (14), we adopt a divide-and-conquer strategy. We first deal with problem (14) by SCP with P fixed, and then find the optimal P by exhaustive search. Now, suppose that the variable P is fixed to a constant \hat{P} . Then, problem (14) can be reformulated into its equivalent, alternative form:

$$\begin{aligned} \min_{\mathbf{F} \in \mathbb{R}^{3M \times N}, \mathbf{H} \in \mathbb{R}^{N \times N}} \quad & \text{Tr}(\mathbf{H}) \\ \text{s.t.} \quad & \mathbf{0} \preceq \text{vec}(\mathbf{F}) \preceq \mathbf{1}_{3MN}, \mathbf{F}\mathbf{1}_N = \hat{P}\mathbf{1}_{3M}, \mathbf{H} \succeq (\mathbf{F}^T \mathbf{\Lambda}_{\hat{P}}^{-1} \mathbf{F})^{-1}, \end{aligned} \quad (16)$$

where the last constraint, linear matrix inequality, can be further rewritten, via Schur's complement [18, Th. 7.7.6, p. 472], as

$$\begin{bmatrix} \mathbf{H} & \mathbf{I}_N \\ \mathbf{I}_N & \mathbf{F}^T \mathbf{\Lambda}_{\hat{P}}^{-1} \mathbf{F} \end{bmatrix} \succeq \mathbf{0}. \quad (17)$$

By letting $\mathbf{U} = \mathbf{F}^T \mathbf{\Lambda}_{\hat{P}}^{-1} \mathbf{F}$, we can write problem (16) as

$$\begin{aligned} \min_{\mathbf{F} \in \mathbb{R}^{3M \times N}, \mathbf{H}, \mathbf{U} \in \mathbb{R}^{N \times N}} \quad & \text{Tr}(\mathbf{H}) \\ \text{s.t.} \quad & \mathbf{0} \preceq \text{vec}(\mathbf{F}) \preceq \mathbf{1}_{3MN}, \mathbf{F}\mathbf{1}_N = \hat{P}\mathbf{1}_{3M}, \end{aligned} \quad (18a)$$

$$\mathbf{U} = \mathbf{F}^T \mathbf{\Lambda}_{\hat{P}}^{-1} \mathbf{F}, \quad (18b)$$

$$\begin{bmatrix} \mathbf{H} & \mathbf{I}_N \\ \mathbf{I}_N & \mathbf{U} \end{bmatrix} \succeq \mathbf{0}. \quad (18c)$$

Solving problem (18) is difficult, due to non-convexity of (18b). Next, we seek for local optimization methods that approximate (18b) using first-order Taylor series, so as to make problem (18) able to be solved by a sequence of convex problems. Applying Newton's method [19] to the quadratic matrix equation $Q(\mathbf{F}) = \mathbf{U} - \mathbf{F}^T \mathbf{\Lambda}_{\hat{P}}^{-1} \mathbf{F} = \mathbf{0}$, where $Q: \mathbb{R}^{N \times N} \mapsto \mathbb{R}^{N \times N}$ is a continuously differentiable function, will have the following recurrence

$$\text{given } \mathbf{F}_0 \text{ (initial guess of } \mathbf{F}), \quad (19a)$$

$$\mathbf{U} - \mathbf{F}_k^T \mathbf{\Lambda}_{\hat{P}}^{-1} \mathbf{F}_k = \mathbf{F}_k^T \mathbf{\Lambda}_{\hat{P}}^{-1} \Delta \mathbf{F} + \Delta \mathbf{F}^T \mathbf{\Lambda}_{\hat{P}}^{-1} \mathbf{F}_k, \quad (19b)$$

$$\mathbf{F}_{k+1} = \mathbf{F}_k + \Delta \mathbf{F}, \quad k = 0, 1, 2, \dots \quad (19c)$$

where $\Delta \mathbf{F}$ denotes a small change in \mathbf{F} , and \mathbf{F}_k denotes the estimate of \mathbf{F} at iteration k . The details of how we derive (19) is provided in the SM¹. Since the newly updated \mathbf{F}_{k+1} should be feasible to (18), $\mathbf{F}_k + \Delta \mathbf{F}$ should also fulfill (18a). By replacing the equality constraint (18b) with (19b), at each iteration k , we can obtain the following SDP formulation:

$$\begin{aligned} \min_{\Delta \mathbf{F} \in \mathbb{R}^{3M \times N}, \mathbf{H}, \mathbf{U} \in \mathbb{R}^{N \times N}} \quad & \text{Tr}(\mathbf{H}) \\ \text{s.t.} \quad & \mathbf{0} \preceq \text{vec}(\mathbf{F}_k + \Delta \mathbf{F}) \preceq \mathbf{1}_{3MN}, (\mathbf{F}_k + \Delta \mathbf{F})\mathbf{1}_N = \hat{P}\mathbf{1}_{3M}, \\ & \mathbf{U} - \mathbf{F}_k^T \mathbf{\Lambda}_{\hat{P}}^{-1} \mathbf{F}_k = \mathbf{F}_k^T \mathbf{\Lambda}_{\hat{P}}^{-1} \Delta \mathbf{F} + \Delta \mathbf{F}^T \mathbf{\Lambda}_{\hat{P}}^{-1} \mathbf{F}_k, \end{aligned} \quad (20)$$

\mathbf{H}, \mathbf{U} satisfy (18c).

The above SDP problem can be efficiently solved by any convex optimization solvers [17]. Note that problem (18) is now handled by a sequence of SDPs given by (20). In each iteration k , problem (20) is thought of as a local, linear approximation to problem (18). Once $\Delta\mathbf{F}$ is obtained at the iteration k , we will update \mathbf{F}_{k+1} by (19c), and continue to solve problem (20) for $k := k + 1$.

Since SCP is a local approximation, using the iterative SCP (20) for solving problem (18) may converge to local minima. To reduce the risk of local optima, we empirically impose a penalty term to the objective function, which amounts to the maximum of the off-diagonal elements of the matrix \mathbf{U} ; i.e.,

$$D(\mathbf{U}) = \max_{i \neq j} u_{ij}, \quad (21)$$

where u_{ij} is the (i, j) th element of \mathbf{U} . The idea is motivated by the fact that minimizing the objective function $\text{Tr}(\mathbf{U}^{-1})$ in (14) suffices maximizing $\text{Tr}(\mathbf{U})$, or minimizing $D(\mathbf{U})$, due to the properties $u_{ij} \geq 0$, $\forall i, j$, $\sum u_{ij} = \hat{P}^2 \mathbf{1}_{3M}^T \mathbf{\Lambda}_{\hat{P}}^{-1} \mathbf{1}_{3M}$, and $\mathbf{U} \succ \mathbf{0}$, inferred from (18a)-(18b). The complete SCP for problem (18) is summarized in Algorithm 1. The initial \mathbf{F}_0 should be feasible—the elements of \mathbf{F}_0 are randomly generated following uniform distribution over $[0, 1]$, and are normalized to satisfy (18a). The weight of the penalty function λ is empirically set to $2N/(3\hat{P}M)$. The iteration procedure will stop when the relative change in objective function is smaller than a preset threshold. A convenient implementation of Algorithm 1 using CVX [17] is provided in the SM¹.

Algorithm 1. Sequential convex programming for problem (18).

input : total energy of the multiplexing \hat{P} , the noise covariance matrix $\mathbf{\Lambda}_{\hat{P}}$ given by (10), initial multiplexing codes \mathbf{F}_0 , $\lambda = 2N/(3\hat{P}M)$ and iteration number $k = 0$.

while *not converged* **do**

 solve the linearized convex problem

$$\{\Delta\mathbf{F}^*, \mathbf{H}^*, \mathbf{U}^*\} = \arg \min_{\Delta\mathbf{F}, \mathbf{H}, \mathbf{U}} \text{Tr}(\mathbf{H}) + \lambda D(\mathbf{U}) \text{ s.t. all constraints in (20);}$$

 update $\mathbf{F}_{k+1} = \mathbf{F}_k + \Delta\mathbf{F}^*$ and $k := k + 1$;

end

output: solution $\bar{\mathbf{F}}(\hat{P}) = \mathbf{F}_k$ and optimal value $\bar{J}(\hat{P}) = \text{Tr}(\mathbf{H}^*)$ to problem (16).

The remaining problem is to determine the optimal total energy of the activated light sources P . Once the optimal value $\bar{J}(\hat{P})$ for $\hat{P} = 2, 3, \dots, P_{\text{sat}}$ are obtained by Algorithm 1, where setting P_{sat} given by (6) as an upper bound is to account for saturation problem in multiplexing, the time and color multiplexing matrix \mathbf{F} to problem (14) can be found by $\mathbf{F}^* = \bar{\mathbf{F}}(P^*)$ for

$$P^* = \min_{\hat{P}=2,3,\dots,P_{\text{sat}}} \bar{J}(\hat{P}). \quad (22)$$

3.2 Application of Algorithm 1 to Time Multiplexing

The methodology shown in the above subsection can also be applied to time multiplexing. Recall the time multiplexing model (1), where \mathbf{A} becomes $M \times N$ instead of $N \times N$ conventionally addressed in the previous works [1, 2, 4, 10, 11]. Following the similar derivations in (11), (12), (13) and (14), the design of such $\mathbf{A} \in \mathbb{R}^{M \times N}$ is to solve the optimization problem

$$\begin{aligned} \{\mathbf{A}^*, P^*\} = \arg \min_{\mathbf{A} \in \mathbb{R}^{M \times N}, P \in \mathbb{R}} \text{Tr}((\mathbf{A}^T \boldsymbol{\Sigma}_P^{-1} \mathbf{A})^{-1}) \\ \text{s.t.} \quad \mathbf{0} \preceq \text{vec}(\mathbf{A}) \preceq \mathbf{1}_{MN}, \mathbf{A} \mathbf{1}_N = P \mathbf{1}_M. \end{aligned} \quad (23)$$

Since problem (23) has a similar structure as (14), following Section 3.1, one can apply Algorithm 1 to solve problem (23); see the SM¹ for details.

4 Computer Simulations

The performance of the proposed code design algorithm, in terms of multiplexing gain, will be demonstrated, for time multiplexing, as well as time and color multiplexing in this section. The purpose of showing results with time multiplexing is to make a baseline comparison with the existing algorithms [11, 12].

4.1 Time Multiplexing

There are $N = 24$ distinct illuminations, and $M = 24, 48, 72$ measurements allowed to be captured by using time multiplexing. Two noise parameters given by (2) are set to $\sigma^2 = 1.5$ and $\rho^2 = 0$. Figure 1(a) shows the comparable performance of the proposed method (i.e., Alg1) to Ratner's method [11] for $M = 24$. Next, we further examine the performance of the proposed method to various number of measurements. Since Ratner's method was developed for determined multiplexing system $M = N = 24$, we repeat Ratner's optimal 24×24 multiplexing matrix twice and three times for $M = 48, 72$, respectively. As shown in Figure 1(b), the performance improvement of the proposed method over Ratner's method can be obviously seen as $M > N$, regardless of the value of P . This immediately suggests that if someone demands a high-quality image under single lighting condition, the solution for that is to acquire more number of measurements using the proposed multiplexing codes.

4.2 Time and Color Multiplexing

We consider the time and color multiplexing where there are $N = 24$ disparate illuminations and $M = 8, 16, 24$ number of RGB multiplexed images. Some noise parameters in $\mathbf{\Lambda}_P$ in (10) are set to $\sigma_r^2 = 1.5$, $\sigma_g^2 = 0.9\sigma_r^2$, $\sigma_b^2 = 2\sigma_r^2$, and $\rho_c^2 = \sigma_c^2 \chi^2$, $c \in \{r, g, b\}$, where χ^2 denotes the common ratio of the sensor noise power and photon noise power for RGB channels. Figure 2(a) shows the object to be illuminated. Figure 2(b) is the synthetic map of material colors

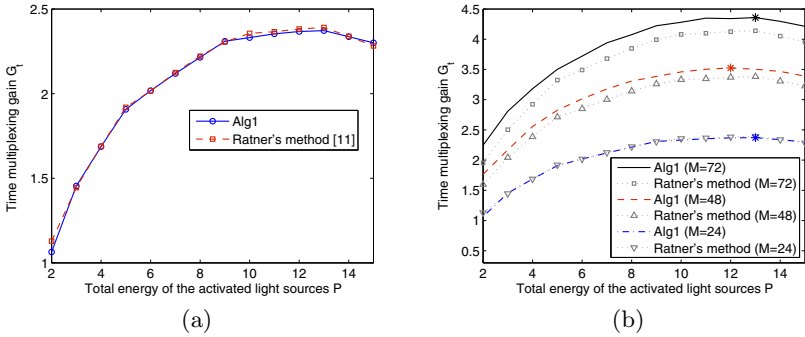


Fig. 1. Time multiplexing for $N = 24$ over various P . (a) shows G_t of the proposed method (Alg1) and Ratner’s method for $M = 24$. (b) shows G_t of the Alg1 and Ratner’s method for $M = 24, 48, 72$, where ‘*’ denotes the maximum G_t for a specific M .

of the object. Figure 2(c) shows the time and color multiplexing gain of the proposed Alg1 for $M = 8, 16, 24$ in the absence of photon noise; i.e., $\chi^2 = 0$. The multiplexing gain improves as the number of measurements M increases. While this observation is similar to time multiplexing shown in Figure 1(b), to maintain the equal multiplexing gain, the number of measurements required by time and color multiplexing is less than time multiplexing by a factor of 3, thanks to three RGB channels utilized for multiplexing. Moreover, the impact of photon noise on the time and color multiplexing is also evaluated in Figure 2(d). It can be seen that the optimal total energy of the activated light sources P^* may decrease when the photon noise goes up, or χ^2 increases. This directly reflects the fact that multiplexing more light sources P results in superposition of more photon noise, and the optimal P should be pulled back in the presence of photon noise.

5 Experiments

We demonstrate the effectiveness of the proposed time and color multiplexing method by object illumination. A PC-controlled BENQ MX761 projector created patterns of $N = 24$ light patches on a white diffuse wall corner. Lights reflected by these patches acted as separate light sources illuminating the placed object—pink piglet, shown in Figure 3(a). A camera FUJINON FL2G13S2C-C was used to capture the multiplexed images, and its exposure time and amplifier gain were set to 150 msec and 0 dB, respectively. The experiment setup, illumination patterns, and some more results are provided in the SM¹.

5.1 Material Colors, Calibration and Noise Estimation

A pre-scan of the object under white light condition is required for estimation of the RGB material colors of the object. Suppose that the RGB values of the

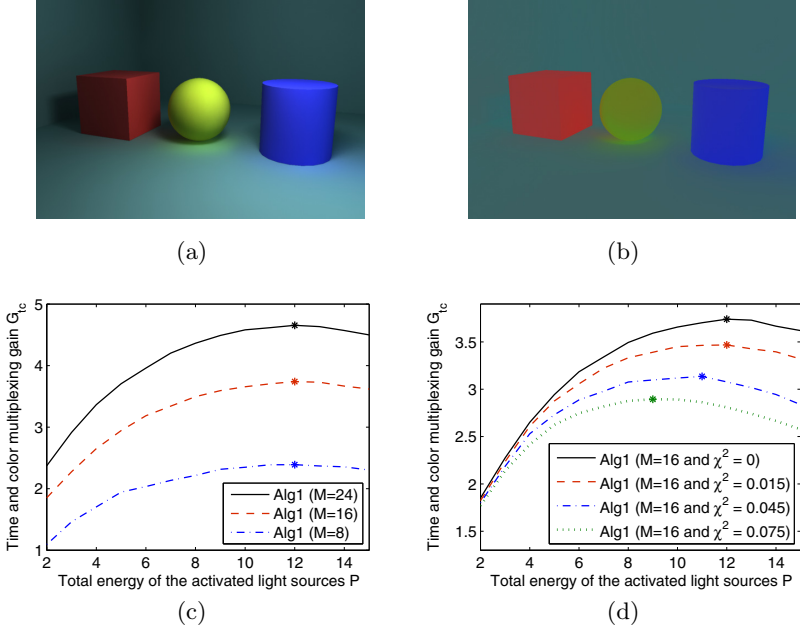


Fig. 2. Time and color multiplexing for $N = 24$ over various P . (a) is the object. (b) is the synthetic map of material colors. (c) shows G_{tc} of the Alg1 for $M = 8, 16, 24$. (d) shows G_{tc} of the Alg1 for $M = 16$ and various χ^2 . The symbol ‘*’ denotes the maximum G_{tc} for a specific setting.

acquired color image are $\{z_r[n]\}_{n=1}^L, \{z_g[n]\}_{n=1}^L, \{z_b[n]\}_{n=1}^L$. Then, the material colors can be calculated by $\alpha_c[n] = z_c[n]/(z_r[n] + z_g[n] + z_b[n]), n = 1, \dots, L, c \in \{r, g, b\}$. The synthetic map of the material colors is shown in Figure 3(b).

Two issues are considered in camera calibration. The first one is the nonlinear effect of the camera readout as the intensity of light source increases linearly. Usual step for fixing this effect is to enable γ -correction mode in the camera, but it is not advised for multiplexing [4]. Instead, we compensate this nonlinearity by assigning nonlinear reference values to projector such that the illuminations measured by the camera are linear in light intensity. Specifically, we use a nonlinear function, $f(x) = \eta x^{1/\gamma}$ where $\eta = 0.98$ and $\gamma = 1.98$, to transform the linear input $x \in [0, 1]$ to a reference value $f(x)$ for projector to display the strength of lighting. The other issue is the spectra overlap among RGB channels of the camera. Since the spectra of red and blue channels are almost disjoint and that of green channel is overlapped with that of red and blue channels, we therefore only use two channels, red and blue, for time and color multiplexing.

In the design of optimal time and color multiplexing codes, the measurement noise variances $\{\sigma_r^2, \sigma_b^2\}$ and photon noise variances $\{\rho_r^2, \rho_b^2\}$ play a central role. We follow the method reported in [11] to estimate the variances of sensor noise and photo noise for red and blue channels of the camera, and the resultant

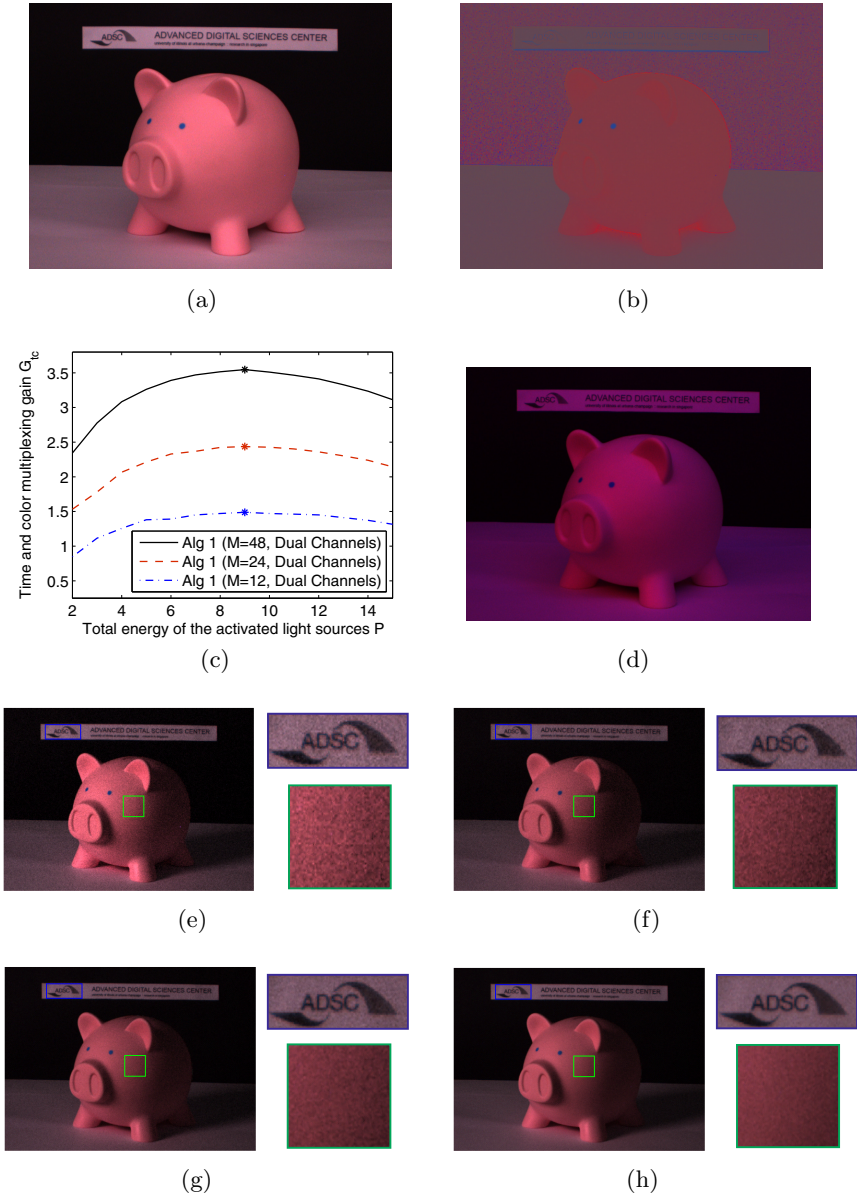


Fig. 3. Experimental results of time and color multiplexing for object illumination. (a) is the object to be illuminated. (b) is the synthetic map of material colors $\{\alpha_r[n], \alpha_g[n], \alpha_b[n]\}_{n=1}^L$. (c) presents the time and color multiplexing gain G_{tc} for $M = 12, 24, 48$, and ‘*’ denotes the maximum G_{tc} for a specific M . (d) represents one of the multiplexed images. (e) is the 12th demultiplexed image via trivial illumination $M = 12, \mathbf{F} = \mathbf{I}_{24}$. (f)-(h) correspond to the 12th single-light source images demultiplexed from 12, 24, 48 time and color multiplexed images, respectively.

variances of sensor noise are $\sigma_r^2 = 0.8033$, $\sigma_b^2 = 1.1238$, and variances of photon noise are $\rho_r^2 = 0.0787$ and $\rho_b^2 = 0.0742$.

5.2 Object Illumination

As the noise variances and the material colors were acquired in the above subsections, the time and color multiplexing codes can be easily computed by using the proposed method in Algorithm 1. Figure 3(c) shows the time and color multiplexing gain G_{tc} for various number of multiplexed images $M = 12, 24, 48$. In this experimental setting, using $M = 48$ and $M = 24$ multiplexed images would have triple and double multiplexing gain improvement in comparison to that using $M = 12$. Figure 3(d) displays one of the multiplexed images, which looks like more dominant in red and blue since only red, blue and their combinations were used for illuminating the object. By demultiplexing from the M multiplexed images, we can obtain the $N = 24$ demultiplexed single-light source illuminations $\{\widehat{\mathbf{s}}[n]\}_{n=1}^L$, which do not contain any color information. We can incorporate the material colors into $\{\widehat{\mathbf{s}}[n]\}_{n=1}^L$ to have the RGB single-light source illuminations, where the intensity of the j th illumination in RGB channels are written as $\{\alpha_c[n]\widehat{s}_j[n]\}_{n=1}^L$, $c \in \{r, g, b\}$. Figures 3(e)-3(h) show the 12th RGB single-light source illuminations obtained from trivial illumination $M = 12$, $\mathbf{F} = \mathbf{I}_{24}$, and from $M = 12, 24, 48$ time and color multiplexed images, respectively. The blue and green marked rectangles are magnified to the right of each image. One can clearly see that the quality of the demultiplexed image, in terms of visual comparison, improves as the time and color multiplexing was used and the number of measurements M increased. For a quantitative analysis, we computed the variances of the signals within a 320×320 square in the black background of these demultiplexed images. These values, referred to as noise variance, are computed as 1.2522, 0.4056, 0.2209, and 0.1563 for trivial illumination, and 12, 24, 48 time and color multiplexed images, respectively, which again confirmed the benefits of using time and color multiplexing and more number of measurements.

6 Conclusions

We have formulated a maximum-SNR code design problem for time and color multiplexing with $M \geq N$, and proposed a sequential SDP approach for handling the formulated problem. The proposed method not only achieves equal performance to Ratner's method [11] for time multiplexing and special case $M = N$, but also opens a new door for a general setting in either time multiplexing, or time and color multiplexing. As deduced from the simulation and experimental results, we summarized the primary merits of the proposed method as below:

- the SNR gain boost for time multiplexing if $M > N$, and for time and color multiplexing if $KM > N$, where K is the number of color channels used;
- the requirement of $1/K$ number of measurements in time and color multiplexing for achieving equal performance when using time multiplexing.

Acknowledgments. The authors wish to thank Mr. Netanel Ratner and Dr. Yoav Y. Schechner for providing the Matlab codes of the method [11]. This study is supported by the research grant for the Human Sixth Sense Programme at the Advanced Digital Sciences Center from Singapore’s Agency for Science, Technology and Research (A*STAR). This work was partially supported by the funding of ONR N00014-09-1-0230, NSF CCF 09-64215, NSF IIS 11-16012, and DARPA KECOM 10036- 100471.

References

1. Harwit, M., Sloane, N.J.A.: Hadamard Transform Optics. Academic Press (1979)
2. Schechner, Y.Y., Nayar, S.K., Belhumeur, P.N.: A theory of multiplexed illumination. In: IEEE International Conf. Computer Vision (2003)
3. Gu, J., Kobayashi, T., Gupta, M., Nayar, S.K.: Multiplexed illumination for scene recovery in the presence of global illumination. In: IEEE International Conf. Computer Vision (2011)
4. Schechner, Y.Y., Nayar, S.K., Belhumeur, P.N.: Multiplexing for optimal lighting. IEEE Trans. Pattern Analysis and Machine Intelligence 29, 1339–1354 (2007)
5. Alterman, M., Schechner, Y.Y., Weiss, A.: Multiplexed fluorescence unmixing. In: IEEE International Conf. Computational Photography (2010)
6. Wenger, A., Gardner, A., Tchou, C., Unger, J., Hawkins, T., Debevec, P.: Performance relighting and reflectance transformation with time-multiplexed illumination. ACM Trans. Graph. (Proc. SIGGRAPH) 24, 756–764 (2005)
7. Kim, H., Wilburn, B., Ben-Ezra, M.: Photometric Stereo for Dynamic Surface Orientations. In: Daniilidis, K., Maragos, P., Paragios, N. (eds.) ECCV 2010, Part I. LNCS, vol. 6311, pp. 59–72. Springer, Heidelberg (2010)
8. Fyffe, G., Yu, X., Debevec, P.: Single-shot photometric stereo by spectral multiplexing. In: IEEE International Conf. Computational Photography (2011)
9. Wagner, A., Wright, J., Ganesh, A., Zhou, Z., Mobahi, H., Ma, Y.: Towards a practical face recognition system: Robust alignment and illumination by sparse representation. IEEE Trans. Pattern Analysis and Machine Intelligence (2012)
10. Wutting, A.: Optimal transformations for optical multiplex measurements in the presence of photon noise. Applied Optics 44, 2710–2719 (2005)
11. Ratner, N., Schechner, Y.Y.: Illumination multiplexing within fundamental limits. In: IEEE Conf. Computer Vision and Pattern Recognition (2007)
12. Ratner, N., Schechner, Y.Y., Goldberg, F.: Optimal multiplexed sensing: bounds, conditions and a graph theory link. Optics Express 15, 17072–17079 (2007)
13. Park, J.I., Lee, M.H., Grossberg, M.D., Nayar, S.K.: Multispectral imaging using multiplexed illumination. In: IEEE International Conf. Computer Vision (2007)
14. Decker, B.D., Kautz, J., Mertens, T., Bekaert, P.: Capturing multiple illumination conditions using time and color multiplexing. In: IEEE Conf. Computer Vision and Pattern Recognition (2009)
15. Liu, C., Freemand, W.T., Szeliski, R., Kang, S.B.: Noise estimation from a single image. In: IEEE Conf. Computer Vision and Pattern Recognition (2006)
16. Fletcher, R.: Practical Methods of Optimization. Wiley, New York (1987)
17. Grant, M., Boyd, S.: CVX: Matlab software for disciplined convex programming, version 1.21 (2011)
18. Horn, R.A., Johnson, C.R.: Matrix Analysis. Cambridge Univ. Press, New York (1985)
19. Higham, N.J.: Newton’s method for the matrix square root. Mathematics of Computation 46, 537–549 (1986)